Dispersion of 4*f* impurity states in photoemission spectra of Yb/W(110)

Yu. S. Dedkov,[*] D. V. Vyalikh, M. Holder, M. Weser, S. L. Molodtsov, and C. Laubschat
Institut für Festkörperphysik, Technische Universität Dresden, 01062 Dresden, Germany

Yu. Kucherenko
Institute for Metal Physics, National Academy of Sciences of Ukraine, 03142 Kiev, Ukraine

M. Fonin
Fachbereich Physik, Universität Konstanz, 78457 Konstanz, Germany

Angle-resolved photoemission spectra of a monolayer of Yb on W(110) reveal energy splittings and dispersion of the Yb 4*f* states at well-defined points of the surface Brillouin zone that are obviously due to hybridization with W-derived valence bands. From the structural incoherence of overlayer and substrate we conclude that the dispersion is not related to the periodic arrangement of the 4*f* states but is due to Yb 4*f* impurities that interact independently with W bands.

In recent years, investigation of heavy-fermion behavior in Ce and particularly Yb systems has attracted renewed interest in the framework of quantum phase transitions.[1,2] As prominent examples, in compounds of the type YbX_2Si$_2$ (X =Rh, Ir) the electronic properties may be tuned from superconductivity to magnetism by replacing the 5*d* element Ir by the isoelectronic 4*d* element Rh.[3,4] The compounds are, thus, thought to be on different sites of a quantum critical point where coexistence of these opposite properties may be expected at zero temperature. The low-temperature magnetic and conducting properties in both compounds are strongly influenced by effective masses of the conduction electrons that are by factor of thousand larger than the one of a free electron due to interactions of the 4*f* states with valence bands. The effective masses relate to the band dispersions that can be studied most directly applying angle-resolved photoemission (PE).

Angle-resolved PE experiments reveal energy splittings and dispersion of the interacting 4*f* states as intuitively may be expected from a Kondo lattice.[5–7] However, these phenomena are not restricted to the region of the Kondo resonance, where the PE final state is energetically degenerated with the 4*f* ground state, but are also observed for 4*f* emission at higher binding energies.[8,9] There, the fully screened PE final state is usually handled like a localized exciton[10] and energy dispersions are at first glance not expected. Interestingly, these phenomena occur around points in reciprocal space where the PE final state becomes energetically degenerated with dispersing valence states. Thus, the basic question arises whether the observed phenomena are necessarily related to a Kondo lattice, i.e., a periodic arrangement of interacting 4*f* states or may also be expected for a single 4*f* impurity interacting with translational symmetric bands.

In order to answer this question, we performed angle-resolved PE experiments of a Yb monolayer on W(110). Divalent Yb grows epitaxially on the W substrate but its two-dimensional hexagonal lattice is incoherent to the rectangular centered substrate surface structure (see inset in Fig. 1). In this case the individual Yb atoms experience distinct chemical surroundings. Thereby, the formally trivalent Yb final

state interacts with the W substrate much stronger than with the divalent Yb neighbors. Therefore, the influence of the periodicity of the Yb overlayer on the local interactions of the Yb final state is expected to be negligible and the final state should behave like an isolated impurity. Surprisingly, the $4f_{7/2}$ emission reveals strong energy splittings and dispersion around the $\bar{\Gamma}$ point of the surface Brillouin zone (SBZ), where no interactions with Yb-derived valence bands are expected but an energy degeneracy with underlying W bands takes place. From the fact that this phenomenon is not observed at other **k** points one can conclude that the effect is not related to an interaction of the incoherent lattices but reflects **k**-dependent interactions of a single Yb impurity with the W bands. The phenomenon is properly described in the framework of the same simple approach to the periodic Anderson model (PAM) that previously had been success-
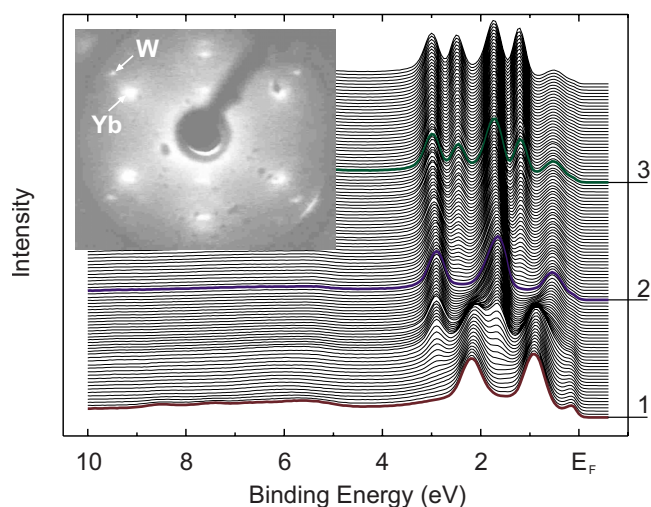

FIG. 1. (Color online) Experimental angle-resolved PE spectra (5° off-normal) obtained during continuous Yb deposition on W(110) surface. Inset shows LEED image of the 1 ML Yb on W(110). LEED spots of Yb and W lattices are clearly visible indicating different symmetry of the overlayer and substrate.

fully applied to the above-mentioned YbX_2Si_2 heavy-fermion systems.[5,6] In this model the unhybridized $4f$ state is represented by a nondispersive band at energy ε that interacts with W derived bands as obtained from a regular band-structure calculation. In the present case the dispersionless $4f$ band is not caused by interatomic f-f interactions, but reflects simply the effect of a Fourier transform of a localized in real-space $4f$ impurity into reciprocal space using basis valence-state wave functions of the substrate lattice. From our data we conclude that the observed $4f$ dispersions in angle-resolved PE spectra are not necessarily the result of a coherent interaction of a periodic arrangement of $4f$ states but may be due to **k**-dependent coupling of independent $4f$ impurities with surrounding valence bands as well.

PE experiments were performed with a hemispherical electron energy analyzer using synchrotron radiation from the U49/2-PGM1 undulator beamline of BESSY (Berlin). The energy resolution was set to 100 meV (full width at half maximum) and an angular resolution better than 1° was used. Structurally ordered films of Yb were grown by vapor deposition at room temperature on a W(110) substrate. Prior to deposition the W surface was cleaned by repeated cycles of heating up to 1300 °C in an oxygen atmosphere at a pressure of 10^{-8} mbar and subsequent flashing up to 2300 °C. Low energy electron diffraction (LEED) patterns of the substrate reveal the sharp pseudohexagonal structure expected for the bcc(110) surface while the LEED pattern of the Yb overlayer shows a hexagonal structure that is incoherent to the one of the substrate and characteristic for the fcc(111) surface of Yb metal (inset in Fig. 1). The base pressure in the vacuum chamber was below 5×10^{-11} mbar, rising shortly to 1×10^{-10} mbar during Yb evaporation. No oxygen contaminations were found in monitoring the O $2p$ photoemission signal.

Yb films reveal strong layer-dependent shifts of the $4f$ emission[11] that may be used to calibrate the thickness of the film and allow for preparation of well defined monolayers. Figure 1 shows a series of angle-resolved PE spectra of the Yb/W(110) system taken for different Yb coverages at 110 eV photon energy and normalized to the maximum of intensity. At this photon energy the W $5d$ emissions are close to a Cooper minimum of the PE cross section[12,13] and the spectra are, therefore, dominated by Yb $4f$-derived emissions. An emission angle of 5° off-normal was chosen in order to eliminate effects that appear close to normal emission and will be discussed later. At a coverage of 1 monolayer (ML) the PE spectrum consists of a single spin-orbit split doublet at 0.91 eV binding energy (BE) superimposed by a flat step-like valence-band background. The spin-orbit splitting amounts to 1.28 eV as characteristic for the $4f$ (Ref. 13) final state of divalent Yb metal.[14] Increasing the Yb coverage, the intensity of this doublet decreases and disappears at coverages exceeding 2 ML. Instead, two new doublets with the same spin-orbit splitting arise at 0.54 and 1.65 eV BE, respectively. Signals at the same BE have been observed previously for a double layer Yb on the isoelectronic Mo(110) surface and were assigned to emissions from interface and surface atoms, respectively.[11] This assignment was supported by thermochemical model calculations that may also be applied to the present case of the Yb/W(110) system since the
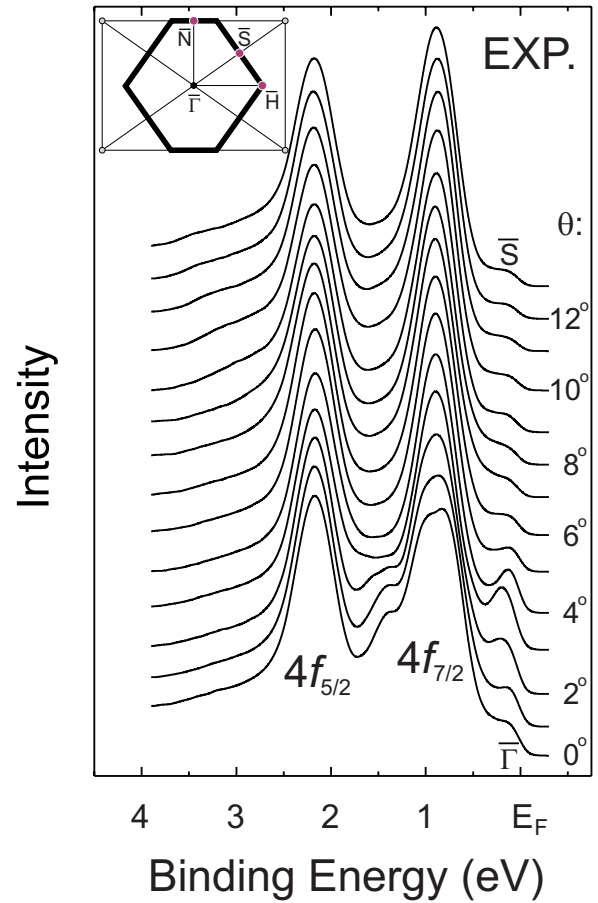

FIG. 2. (Color online) Experimental angle-resolved PE spectra of 1 ML Yb on W(110) surface measured along the $\bar{\Gamma}-\bar{S}$ direction of the W(110) SBZ (thick line in the inset). The corresponding emission angles are marked on the right-hand side of the figure. Note that the linewidth is not limited by the instrumental resolution of 100 meV.

relevant material parameters of Mo and W are almost the same. For coverages exceeding 2 ML the interface component at 0.54 eV BE becomes successively replaced by a new doublet at 1.21 eV that is characteristic for the bulk emission of Yb metal,[11,14] while the BE of the surface component shifts at the same time slightly from 1.65 to 1.73 eV.

In the following we will concentrate on the monolayer Yb on W(110). Figure 2 shows a series of angle-resolved PE spectra taken at different emission angles along the $\bar{\Gamma}-\bar{S}$ direction (inset in Fig. 2) of the SBZ of W(110) and 110 eV photon energy. While at high emission angles only the $4f$ (Ref. 13) doublet is visible in the spectra; additional spectral features appear around normal emission that at first glance might be ascribed to residual valence-band emissions. On the other hand, the spectra can obviously not be explained by a simple superposition of $4f$ and valence-band contributions, since the $4f_{7/2}$ component becomes broadened and decreases in height with respect to the $4f_{5/2}$ emission.

This is illustrated in Fig. 3(a) where spectra taken at emission angles of 0° and 7° are compared to each other together with the results of a least-squares fit analysis. In the framework of this analysis, first the spectrum taken at 7° was fitted
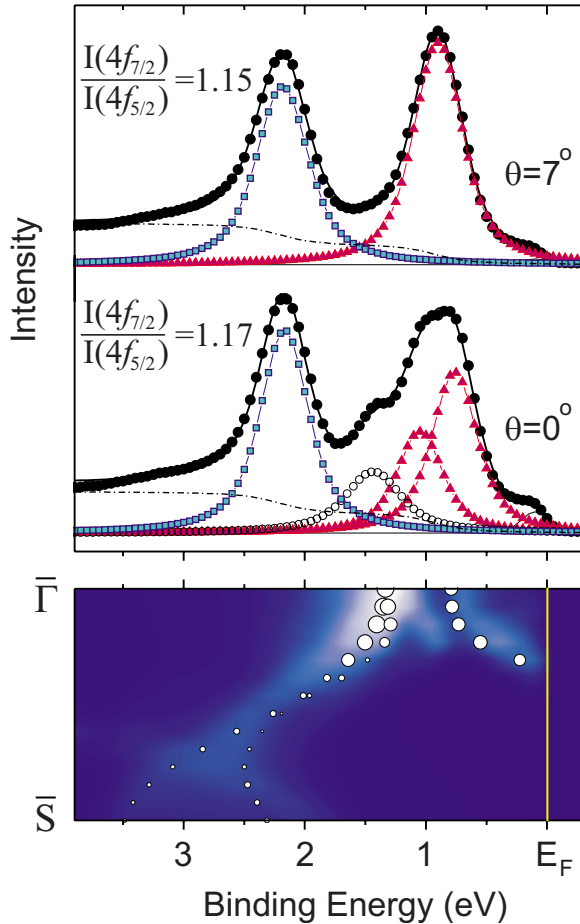
FIG. 3. (Color online) Upper panel: Results of the least-squares fit of experimental PE spectra of 1 ML Yb on W(110) surface collected at emission angles $\theta=0°$ and $7°$. Subspectra: ▲–Yb $4f_{7/2}$, ■–Yb $4f_{5/2}$. Lower panel: Experimental angle-resolved PE data (color plot) and results of the band-structure calculations (white circles) for W(110) measured along the $\bar{\Gamma}-\bar{S}$ direction of the W(110) SBZ. Size of the circles corresponds to the weight of W $5d$ states in valence band.

by a superposition of two Lorentzians with the same linewidth and a $I(4f_{7/2})/I(4f_{5/2})$ intensity ratio of 1.15 ± 0.02 was obtained. Then, the normal-emission spectrum was fitted using four Lorentzians with the same linewidth as used above, replacing the former $4f_{7/2}$ line by components at 1.43, 1.04, and 0.76 eV BE. Taking now the intensity ratio of the last two components with respect to the $4f_{5/2}$ line, almost the same value 1.17 ± 0.02 is obtained as for the $I(4f_{7/2})/I(4f_{5/2})$ intensity ratio of the 7° spectrum. Thus, one might assume that these two components are derived from the former $4f_{7/2}$ line and the third component at 1.43 eV BE represents a valence-band emission. A possible candidate for the latter is the $5d$ band of the underlying W substrate that reveals particularly strong emissions at 1.35 eV BE around the $\bar{\Gamma}$ point and may also be responsible for the features close to the Fermi energy observed at higher emission angles.

Such an interpretation, however, is not fully satisfactory since it does not explain the splitting of the $4f_{7/2}$ component. A similar splitting has been observed for the Ce "$4f^0$" signal

of Ce/W(110) at a point in **k** space where the "$4f^0$" state becomes energy degenerate with the Ce-derived sd band.[8] There, the splitting could be described in the light of the periodic Anderson model by formation of symmetric and antisymmetric linear combinations of wave functions of $4f$ and valence-band states. In the present case of the Yb/W(110) interface, band-structure calculations show[15] that the bottom of the Yb $6s$-derived valence band is located at around 4 eV BE and a crossing of the Yb $4f_{5/2}$ energy position is expected only close to the $\bar{S}$ point. There, however, no hints of a line splitting are observed, which may be explained by the properties of the valence-band states that are in the case of Yb much more localized than in Ce and reveal almost entirely Yb $6s$ character that does not hybridize with the Yb $4f$ states.

If interactions with the Yb valence band can be ruled out as a reason for the $4f$ splitting at the $\bar{\Gamma}$ point, there remain only interactions with the W $5d$ band as an explanation. Similar effects have not been observed for Ce/W(110),[8] possibly because the linewidth and BE of the Ce $4f^0$ state are much larger than for the Yb $4f_{7/2}$ component. In order to describe the interaction with the W band in spite of the lattice mismatch in the framework of the PAM one has to consider the Yb $4f^{13}$ hole states as impurities that interact particularly with W $5d$ out-of-plane states of the W(110) surface. In order to determine the respective characters of the W bands, band-structure calculations have been performed using the linear muffin-tin orbital (LMTO) method.[16] The results are shown by white dots in the lower panel of Fig. 3 where the size of the dots is a measure for the magnitude of the $5d$ weights to the respective valence-band states. [Experimental angle-resolved PE data for W(110) measured along the $\bar{\Gamma}-\bar{S}$ direction are superimposed as a color plot.] Strong $5d$ admixtures to the W bands correspond to strong intensities in the PE signal as is expected from the larger cross section of the W $5d$ as compared to the W $6s$ states. The interaction with the $4f$ state in the light of the PAM may now be handled in a similar way as for the Ce/W(110) system and the YbX_2Si$_2$ heavy-fermion compounds. The unhybridized hole state is considered as a dispersionless band at energy $\varepsilon=\varepsilon(\mathbf{k})$, where the lack of dispersion indicates that in spite of their periodic arrangement the $4f$ states behave essentially independent from each other. Note that also band-structure calculations predict a bandwidth of only 50 meV. The hybridization matrix element $V_{\mathbf{k}}(E)$ is expressed by the amplitude of W $5d$ out-of-plane wave functions $c_d(E,\mathbf{k})$ multiplied by a constant Δ that accounts for the hopping probability. Using the Anderson formalism in hole representation and excluding double-hole states ($4f^{12}$ configurations) from our consideration by setting the on-site Coulomb correlation energy U_{ff} to infinity allows then for a diagonalization of the Hamiltonian. The obtained result is reminiscent of that of the single impurity Anderson model (SIAM). The important difference is, however, that now **k** dependence is achieved by replacing the density of states (DOS) used in the SIAM by **k**-resolved partial weights. Since ε is given by the BE of the $4f_{7/2}$ component at **k** points far away from the $\bar{\Gamma}$ point the proportionality constant Δ (equal to 0.22 eV in accordance with our earlier works on Yb systems) is the only adjustable param-

eter of this approach. The plot of $V_{\mathbf{k}}(E)$ can be expressed from Fig. 3 (lower panel), where the W 5d weight of the valence-band states of W is shown. The states with a large W 5d contribution will have larger $c_d(E,\mathbf{k})$ and in this case this plot can be taken as a plot of $V_{\mathbf{k}}(E)$ in the PAM because Δ is a constant. In the case of the SIAM the **k**-averaged hybridization is a constant for all **k** vectors over the whole BZ.

Figure 4 shows a series of calculated 4f spectra along the $\bar{\Gamma}-\bar{S}$ direction of the W(110) SBZ that reproduces all features observed in the respective experimental data. Note that particularly the peak at 1.37 eV BE in the normal-emission spectrum should not be considered as a pure valence-band emission but represents a hybrid state with strong 4f admixture. Since in the calculations only the 4f character is shown, its intensity relative to the unhybridized 4$f_{5/2}$ component is weaker than in the experiment. Similar arguments hold for the features close to the Fermi energy that are caused by hybridization of the 4$f_{7/2}$ state with an upward dispersing band. Note that also for the 4$f_{5/2}$ state an intersection with the band is expected from dispersion. This takes place halfway between the $\bar{\Gamma}$ and $\bar{S}$ points, and in fact the model calculations reveal a change in the 4$f_{5/2}$ line shape. This change, however, is very weak because the d admixture to the valence-band state is small and this effect is beyond the experimental resolution.

In summary, we have shown that the Yb 4f PE signals of Yb/W(110) reveal energy splittings and dispersions that are caused by hybridization of the Yb 4f states with W 5d-derived bands. These effects appear at well defined points in reciprocal space although the 4f states are expected to behave as independently interacting impurities due to the incoherence of the lattices of Yb and W. Thus, the observed 4f dispersions are obviously an effect of the interaction of the 4f impurities with dispersing W 5d valence bands and the periodicity of the Yb lattice is not important. Applying this result to heavy-fermion systems one may conclude that the observation of 4f dispersions in angle-resolved PE experiments is not necessarily a proof for f-f interactions within a
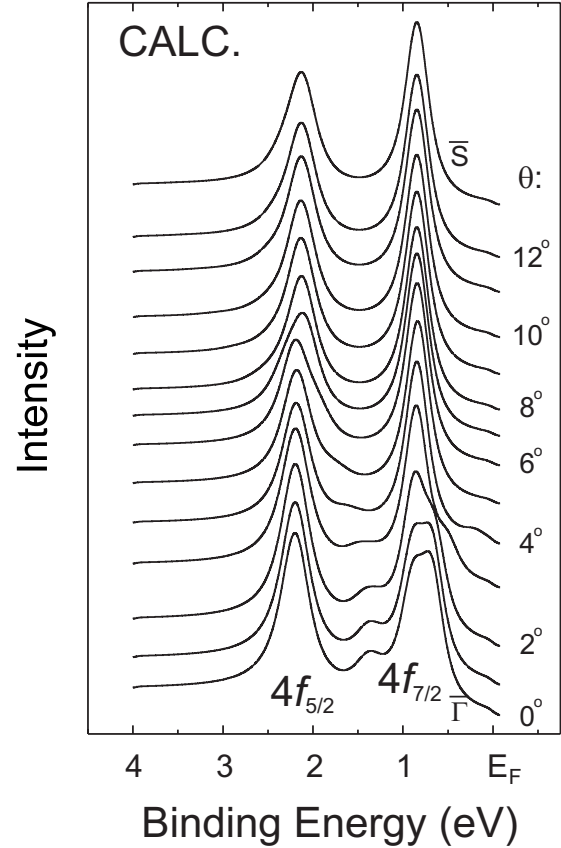

FIG. 4. Calculated angle-resolved PE spectra of 1 ML Yb on W(110) along the $\bar{\Gamma}-\bar{S}$ direction of the W(110) SBZ.

Kondo lattice but might be caused by Kondo impurities independently interacting with itinerant electrons as well.

*Corresponding author. Present address: Fritz-Haber Institut der Max-Planck Gesellschaft, 14195 Berlin, Germany; dedkov@fhi-berlin.mpg.de

[1] S. Sachdev, Nat. Phys. **4**, 173 (2008).

[2] P. Gegenwart, Q. Si, and F. Steglich, Nat. Phys. **4**, 186 (2008).

[3] O. Trovarelli, C. Geibel, S. Mederle, C. Langhammer, F. M. Grosche, P. Gegenwart, M. Lang, G. Sparn, and F. Steglich, Phys. Rev. Lett. **85**, 626 (2000).

[4] Z. Hossain, C. Geibel, F. Weickert, T. Radu, Y. Tokiwa, H. Jeevan, P. Gegenwart, and F. Steglich, Phys. Rev. B **72**, 094411 (2005).

[5] S. Danzenbächer, Y. Kucherenko, M. Heber, D. V. Vyalikh, S. L. Molodtsov, V. D. P. Servedio, and C. Laubschat, Phys. Rev. B **72**, 033104 (2005).

[6] S. Danzenbächer, Yu. Kucherenko, D. V. Vyalikh et al., Phys. Rev. B **75**, 045109 (2007).

[7] D. V. Vyalikh, S. Danzenbächer, A. N. Yaresko et al., Phys. Rev.

Lett. **100**, 056402 (2008).

[8] D. V. Vyalikh, Yu. Kucherenko, S. Danzenbächer, Yu. S. Dedkov, C. Laubschat, and S. L. Molodtsov, Phys. Rev. Lett. **96**, 026404 (2006).

[9] S. Danzenbächer, Yu. Kucherenko, C. Laubschat et al., Phys. Rev. Lett. **96**, 106402 (2006).

[10] B. Johansson, Phys. Rev. B **20**, 1315 (1979).

[11] N. Mårtensson, A. Stenborg, O. Björneholm, A. Nilsson, and J. N. Andersen, Phys. Rev. Lett. **60**, 1731 (1988).

[12] J.-J. Yeh and I. Lindau, At. Data Nucl. Data Tables **32**, 1 (1985).

[13] S. L. Molodtsov, S. V. Halilov, V. D. P. Servedio, W. Schneider, S. Danzenbacher, J. J. Hinarejos, M. Richter, and C. Laubschat, Phys. Rev. Lett. **85**, 4184 (2000).

[14] W.-D. Schneider, C. Laubschat, and B. Reihl, Phys. Rev. B **27**, 6538 (1983).

[15] Yu. Kucherenko (unpublished).

[16] O. K. Andersen, Phys. Rev. B **12**, 3060 (1975).